

## Time dependent changes in extreme ultraviolet reflectivity of Ru mirrors from electron-induced surface chemistry

A. Kanjilal,<sup>1,a)</sup> M. Catalfano,<sup>1</sup> S. S. Harilal,<sup>1</sup> A. Hassanein,<sup>1</sup> and B. Rice<sup>2</sup>

<sup>1</sup>Center for Materials Under Extreme Environment, School of Nuclear Engineering Purdue University, West Lafayette, Indiana 47907, USA

<sup>2</sup>SEMATECH Inc., Albany, New York 12203, USA

(Received 30 December 2011; accepted 4 February 2012; published online 26 March 2012)

Time dependent changes in 13.5 nm extreme ultraviolet (EUV) reflectivity of Ru mirrors due to variations in surface composition were investigated. The surface properties of Ru films were analyzed *in situ* by means of X-ray photoelectron spectroscopy (XPS), and further verified by Auger electron spectroscopy (AES). Moreover, the impact on EUV reflectivity (EUVR) with time was examined *in situ* via continuous and/or discrete EUV exposures. The rapid decrease in EUVR was observed in the presence of photoelectrons (PEs) from Ru mirror of the EUV setup, whereas no significant variation was recorded by screening out additional PEs. Detailed XPS and AES analyses suggest that carbon deposition via dissociation of residual hydrocarbons plays a dominant role in the presence of additional PEs, and thus reduces the reflectivity rapidly. Using EUV photoelectron spectroscopy, systematic reduction of the secondary electron yield from the Ru mirror surface was observed in consecutive scans, and therefore supports the formation of carbonaceous Ru surface in the presence of additional PEs. © 2012 American Institute of Physics. [<http://dx.doi.org/10.1063/1.3691604>]

### I. INTRODUCTION

In order for semiconductor manufacturing to keep pace with Moore's Law, the development of new optical lithography processes is essential. Current techniques utilize the 193 nm wavelength laser radiation,<sup>1</sup> which at present has reached its physical feature size limit. Next generation processes have been targeted in the extreme ultraviolet (EUV) regime, e.g., 13.5 nm wavelength (due to the existence of reflective mirrors),<sup>2</sup> and thus experimental campaigns to develop such sources<sup>3</sup> and understand the performance of related optics are currently underway worldwide. Both single- and multi-layer mirrors are being considered for EUV optics, where Ru is an excellent candidate either as a primary mirror<sup>4-6</sup> or as a capping layer for multi-layer Mo/Si mirrors.<sup>2</sup> Research suggests that mirror performance and lifetime depend on several variables, such as radiation, chemical exposure, morphology, temperature, etc.<sup>2,7</sup> Among these, chemical changes of the Ru-mask surface are the primary driving force in mirror degradation.<sup>2</sup> In fact, radiation induced carbon contamination and surface oxidation have been shown to drive down mirror reflectivity by theoretical modeling<sup>4</sup> and experiments.<sup>8</sup> Further research indicates that the adsorption and subsequent EUV-induced dissociation of water molecules on Ru surface affect mirror performance,<sup>2</sup> whereas resist outgassing of common hydrocarbons in the vacuum system is a possible source of carbon.<sup>8</sup> In fact, secondary electrons (SEs) from Ru capping layer are known to play a decisive role in contaminating the surface.<sup>2</sup>

Since several mirrors will be used in an EUV lithography (EUVL) setup,<sup>9</sup> a loss of mirror reflectivity by 1%

implies substantial reduction in throughput of the system.<sup>10</sup> Although electron-assisted deposition of carbon on Ru surface has been studied recently<sup>10</sup> to mimic the EUV-induced surface chemistry, the effect of photoelectrons (PEs) on successive mirror reflectivity has not yet been evaluated so far. In particular, the emitted PEs are expected to reach from one mirror to another along with EUV photons. It is, therefore, important to understand the consequence of PEs on the successive mirror reflectivity when the partial pressure of water vapor in the chamber is of the order of  $10^{-7}$  Torr, as future commercial EUV system may not support baking an ultra-high vacuum (UHV) chamber to avoid degradation of the Mo/Si optics performance.<sup>2</sup>

In this article, we show how PEs from a focusing Ru mirror of the EUV setup can deteriorate the EUV reflectivity (EUVR) of a Ru mirror if the partial pressure of water vapor in the chamber is high enough with respect to other constituents. More precisely, we show how the electronic structure of sputter cleaned Ru surface is modified by EUV radiation in the presence and absence of PEs from the focusing mirror, and the corresponding effect on mirror reflectivity. We show a rapid *decrease* in EUVR in time if the additional PEs are not screened out from the EUV light. The observed phenomena have been discussed in the light of additional PE enhanced deposition of carbon atoms via dissociation of residual hydrocarbons on Ru mirror surface using X-ray photoelectron spectroscopy (XPS) and Auger electron spectroscopy (AES) analyses, and further supported by EUV photoelectron spectroscopy (EUPS).

### II. EXPERIMENTAL

The experiments were performed at the materials characterization laboratory IMPACT at CMUXE, which contains

<sup>a)</sup>Electronic mail: akanjilal@purdue.edu.

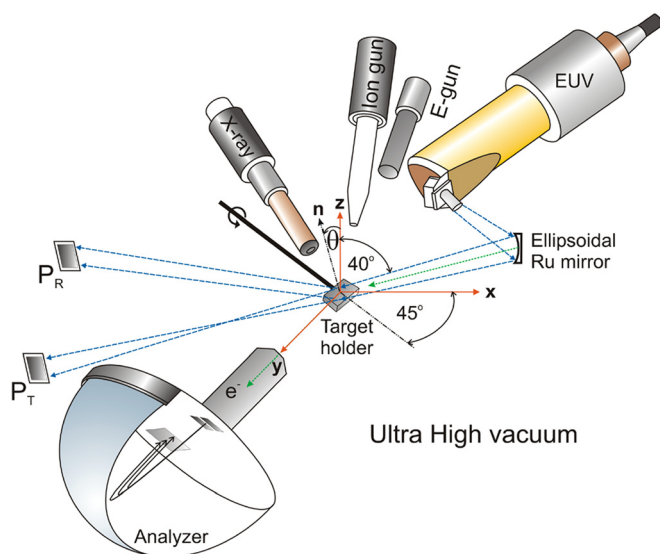


FIG. 1. (Color online) Schematic diagram of the experimental setup.

an UHV chamber equipped with a suite of *in situ* diagnostic tools for surface analysis including XPS, AES, EUPS, low-energy ion scattering spectroscopy, and EUVR (schematically demonstrated in Fig. 1). To create a chamber condition similar to that of EUVL system,<sup>2,9</sup> we did not bake the UHV chamber giving a base pressure of  $\sim 1.8 \times 10^{-8}$  Torr. The residual gas analyzer (RGA-100) reveals a partial pressure of water on the order of  $\sim 2.2 \times 10^{-9}$  Torr with respect to nitrogen, as well as different background hydrocarbons such as methane, acetone, ethyl alcohol, methyl alcohol, benzene, toluene, and methane in conjunction with hydrogen. The XPS measurements at different stages of our experiments were performed using an Al- $K_{\alpha}$  radiation source ( $h\nu = 1486.65$  eV) where the PEs emitted at  $45^{\circ}$  from the target surface were analyzed with a SPECS Phoibos-100 hemispherical electron analyzer having an energy resolution of 0.85 eV. Calibration of binding energy (BE) scale with respect to the measured kinetic energy (KE) was made using silver Fermi edge. A SPECS electron gun situated at an angle of  $65^{\circ}$  from target surface was used for AES measurements. Grazing incidence EUVR has been investigated with the help of Phoenix EUV source<sup>11</sup> that emits light in the range of 12.5–15 nm with peak maximum at  $\sim 13.5$  nm (92 eV), and two calibrated EUV photodiodes (PDs) from International Radiation Detectors Inc.—namely reflecting-PD ( $P_R$ ) and through-PD ( $P_T$ ) as shown in Fig. 1. The target holder is insulated from the chamber and the sample current was measured from the target in series with a grounded Keithley-6487 pico-ammeter. The error in the measured reflectivity was found to be within  $\pm 4\%$ .

The 92 eV photons from the compact EUV source are projected onto the Ru target with the help of an ellipsoidal Ru mirror (see Fig. 1) situated  $\sim 53$  cm away from the target surface. Since this mirror is also used to remove stray X-rays and the Bremsstrahlung radiation from the EUV source,<sup>12</sup> it is also generating PEs. The focusing Ru mirror itself is, however, not subjected to electron bombardment, in contrast to the Ru surface studied. To screen out excess PEs from the

focusing Ru mirror, a magnet has been used to deflect them from the EUV ray path, showing a drastic change in the sample current from  $-0.6$  nA to  $0.5$  nA. In order to understand the effect of the excess PEs on the target reflectivity, EUVR data has been recorded both in presence and with screening out additional PEs.

To carry out our experiments, a 50 nm thick Ru film was grown on *p*-type Si(100) wafer and was diced into several pieces with an average area of  $1 \times 1$  cm<sup>2</sup>. The target surface was sputter cleaned by 2 keV Ar<sup>+</sup> for 15 min (optimized) with beam current of  $\sim 410$  nA. The cleanliness of the Ru surface was monitored *in situ* by XPS and AES. These techniques were further employed to assess the contamination level under EUV exposure. Prior to examining EUVR, the beam was adjusted in such a way that the Ru target can provide maximum intensity in reflecting-PD with a spot size as big as the investigating area.

### III. RESULTS AND DISCUSSION

Electron spectroscopy is a standard technique for monitoring surface composition. At different stages of experiments, the surface composition has been examined by XPS and AES measurements. The impact of surface contamination on EUVR has also been studied, while EUPS is used to confirm the conclusion derived from the XPS and AES studies. We will discuss the results derived from these experiments and draw conclusions from our analyses.

#### A. X-ray photoelectron spectroscopy

Typical XPS spectra of a Ru film are shown in Fig. 2 before (a) and after (b) sputter cleaning, and after EUV exposure for an hour in absence (c), and in the presence (d) of PEs from the focusing Ru mirror. One can see that although the intensity of O 1s (indicated by downward arrow), peaking at 532.9 eV drops after sputter cleaning, it does not change much after EUV exposure with and without the additional PEs. The characteristic Ru peaks have been identified

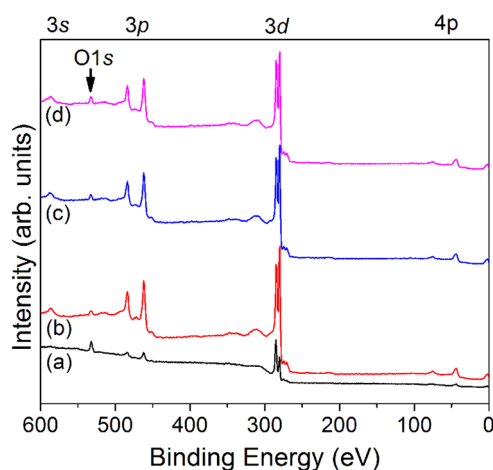


FIG. 2. (Color online) Typical XPS spectra of Ru film before (a) and after (b) sputter cleaning, and after EUV exposure for an hour in absence (c) and presence (d) of PEs from the focusing Ru mirror. The characteristic Ru peaks have been identified and marked as 3s, 3p, 3d, and 4p, where O 1s peak in marked by downward arrow.

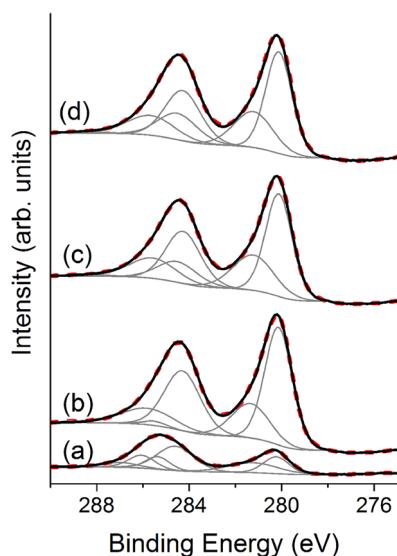


FIG. 3. (Color online) Typical high-resolution XPS spectra of a Ru film before (a) and after (b) sputter cleaning, and after EUV exposure for an hour in absence (c) and presence (d) of PEs from the focusing Ru mirror. The fitting components are shown by the lines in gray, with the final fit in black. Original data are shown by thick dashed lines.

and marked as  $3s$ ,  $3p$ ,  $3d$ , and  $4p$  (Fig. 2), in good agreement with literature.<sup>13</sup> Close inspection of the Ru  $3d$  level (see Fig. 3) reveals that the magnitude of the Ru  $3d_{5/2}$  peak intensity becomes dominant over the adjacent Ru  $3d_{3/2}$  just after sputter cleaning. It is, however, difficult to follow the Ru  $3d_{5/2}$  and  $3d_{3/2}$  peaks before and after sputtering, as Ru  $3d_{3/2}$  evolves in proximity to the C  $1s$  (284.5 eV).<sup>7</sup> To understand the relative changes in carbon concentration in different stages of our experiments due to radiation-induced dissociation of hydrocarbons,<sup>2,14,15</sup> it is essential to identify the Ru  $3d_{5/2}$  and  $3d_{3/2}$  components using conventional fitting procedures. Careful analysis reveals that each of the detected Ru  $3d_{5/2}$  and  $3d_{3/2}$  peaks contains information of both Ru and RuO<sub>2</sub> where the corresponding components are found to be situated at 279.7 eV/280.4 eV and 283.9 eV/284.4 eV, respectively.<sup>7</sup> Moreover, the Ru/C components, which appear between 280 and 290 eV, were fitted systematically using CASA-XPS not only to follow the level of carbon contamination, but also to identify the relative change in peak area intensity of the oxidation states of Ru  $3d_{5/2}$  and  $3d_{3/2}$  during EUV exposures with and without screening of the additional PEs. Typical fitting components are shown in Fig. 3 for convenience, while fitting details are given in Table I. The constrains such as full-width at half maximum

(FWHM), peak positions of underlying components, and intensity (area) ratio of Ru  $3d_{3/2}/3d_{5/2}$  as 2/3 (Ref. 16) are applied to compare the relative change in peak area intensity. A Voigt function consisting of 70% Lorentzian and 30% Gaussian components was employed for the fitting process.

Since the sputter cleaned Ru films show the existence of oxygen on Ru surface, we cannot neglect the adsorption of oxidized forms of carbon on the Ru surface, especially carbon monoxide<sup>17,18</sup> (CO) from residual gases.<sup>15</sup> Hence, the high-resolution XPS spectrum near C  $1s$  region was deconvoluted by six components after subtracting the background (Fig. 3). Although reactive CO adsorbed on Ru(0001) surface would be more stable in the top site position via O-induced lateral weakening of Ru-Ru bonds,<sup>17</sup> we believe that the probability to occupy the hollow sites by adsorbed CO on sputter cleaned Ru surface would be higher than on-top position, and thus give a peak at 285.7 eV similar to Pd (Ref. 19) and Ni (Ref. 20) surfaces. Detailed analysis suggests about  $\sim 5\%$  decrease in metallic Ru (Ru<sup>0</sup>) after screening the additional PEs from the incident EUV light, while the relative peak area intensity of C is increased by  $\sim 1\%$  (Table I). On the other hand, the relative peak area intensity of carbon is increased by  $\sim 4\%$  in the presence of PEs from the focusing Ru mirror, whereas Ru<sup>0</sup> is reduced by  $\sim 7\%$  (see Table I). The FWHM of the Ru  $3d_{5/2}(3d_{3/2})$  of the RuO<sub>2</sub> was found to be larger than that of the respective components for Ru<sup>0</sup>, which is most likely associated with the thickness of the oxidized layer near the surface.<sup>21</sup>

## B. Auger electron spectroscopy

In an attempt to check the consistency of our XPS results (Table I), we have also monitored the corresponding AES spectra *in situ* using 2 keV electron beam (Fig. 4). Although the Auger processes occur for all elements, this technique is especially suitable for the lighter elements (except for hydrogen and helium because of having no or insufficient outer electrons) than the heavier ones,<sup>22</sup> allowing a more sensitive approach to measuring carbon buildup on Ru surface. Because of the peaks in the recorded AES spectra are situated on a high background (left panel), arising from the creation of a large number of SEs due to inelastic scattering processes,<sup>22</sup> all the spectra were differentiated (right panel) for in-depth analyses (Fig. 4). When assigning peaks for the sputter cleaned Ru surface, first we verified the existence of other Auger peaks of Ru situated in the range of 200–274 eV.<sup>23</sup> In the  $dN/dE$  mode (right panel), although

TABLE I. XPS fitting parameters showing relative peak area intensity of carbon, carbon monoxide, Ru<sup>0</sup>, and RuO<sub>2</sub>.

Specifications	Experimental conditions	XPS analyses			
		C (%)	CO (%)	Ru $3d$	
				Ru <sup>0</sup> (%)	RuO <sub>2</sub> (%)
Relative peak area intensity	After sputter cleaning	9.63	1.11	63.65	25.60
	After EUV only	10.49	0.64	58.20	30.68
	After EUV with electrons	13.09	0.71	56.67	29.53

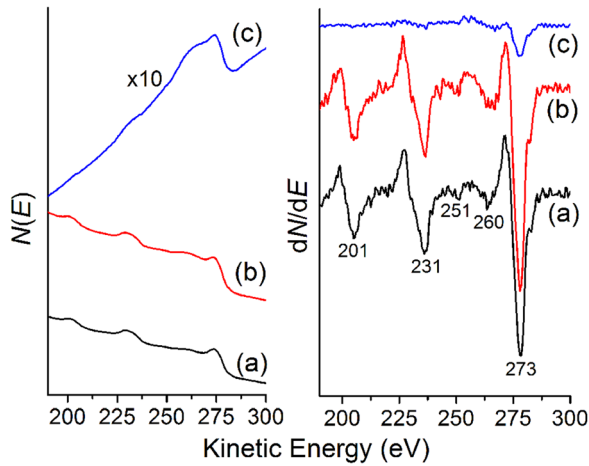


FIG. 4. (Color online) AES Spectra: Left and right panels are showing  $N(E)$  vs KE, and  $dN/dE$  vs KE modes, respectively; AES spectra of Ru film after sputter cleaning (a), and after EUV exposure for an hour by screening out (b) and in the presence (c) of PEs from the focusing Ru mirror. The curve (c) in the left panel is multiplied by 10 for clarity.

the Ru peaks residing at 201 eV ( $M_{45}N_1N_{45}$ ) (Ref. 23) and 231 eV ( $M_{45}N_{23}N_{45}$ ) (Ref. 23) are not interfering with the six possible C *KLL* lines with energies in the range of 243 to 267 eV (depending on the chemical surroundings),<sup>24</sup> the strong Ru( $M_5N_{45}N_{45}$ ) peak<sup>25,26</sup> at 273 eV overlaps with the C *KLL* transition at 272 eV (Refs. 26 and 27–29) and thus makes the matter complicated. However, surface carbon can change the peak-to-peak height as well as the shape of the 273 eV Ru/C line, because the surface sensitivity of an Auger peak is associated with electron mean free path or escape depth ( $\lambda$ ) of the element involved,<sup>30</sup> specifically the KE range of the Auger electrons, and the energy and angle of incidence of the primary beam.<sup>22</sup> In fact, the Auger electron yield relies on several parameters such as ionization cross-section, Auger decay probability, atomic mass and density, and the attenuation length along with the detection efficiency of the electron spectrometer and detector.<sup>23,30</sup> The negative going peak at 273 eV becomes asymmetric and dominates with increasing carbon coverage,<sup>28</sup> while the graphitic and carbidic forms of carbon show different behavior in the range of 250 to 260 eV.<sup>27</sup> As discerned, the Ru Auger signals become weaker after the target was exposed to EUV light in the presence of additional PEs (right panel, Fig. 4), indicating severe contamination of the Ru surface. One can also notice a change in the background of the AES spectra, especially after EUV exposure with additional PEs (left panel,

Fig. 4). Clearly, the change in slope of the background from negative to positive is a fingerprint of increasing surface contamination.

The fine structures near  $\sim 251$  and 260 eV are also prominent in Fig. 4 (right panel). According to Refs. 27 and 28, these fine structures with the main negative-going peak at 273 eV are most likely associated with the carbidic form of carbon. Although there is no confusion in assigning the peak at 260 eV as a carbidic phase of carbon,<sup>31</sup> the positive-going hump near 251 eV with a broad negative-going peak at  $\sim 273$  eV can also be a signature of the graphitic form of carbon.<sup>27</sup> Hence, the systematic increase in Auger peak-to-peak value at 251 eV by suppressing the Ru 231 eV with increasing surface contamination (Fig. 4) is not straightforward. Goodman and White,<sup>28</sup> however, used the peak-to-peak height ratio of the C(251 eV) and Ru(231 eV) as a measure of the level of carbon contamination. As in our sample, carbon is supplied onto the sputter cleaned Ru surface via dissociation of hydrocarbons,<sup>2,14,15</sup> any form of carbon can exist on the Ru surface. Since the peak-to-peak amplitude, especially the negative-going portion of the C 251 eV peak was found enhancing not in proportional to the peaks at 260 and 273 eV with increasing surface contamination, the Auger signal at 251 eV cannot be explained in the framework of the formation of carbidic phase, instead it represents one of the few carbon peaks<sup>24</sup> that is not associated with Ru, possibly graphitic form of carbon.

For determining the level of adsorbed carbon on the Ru target surface, three standard procedures have been used, where the results are summarized in Table II. First, the increase in ratio of the peak-to-peak values of the combined Ru and C signals at 273 eV to Ru 231 eV shows an increase of carbon coverage. The second method involves the comparison of the top part of the 273 eV peak to the bottom part. Because the growth of carbon causes the negative peak to grow, it gives an overall decrease in ratio. The final method involves measuring the ratio of peak-to-peak intensity at 251 eV with that of the pure Ru peaking at 231 eV.<sup>28</sup> All results show that there is a slight increase of carbon while screening out extra PEs, but it is far more pronounced after exposing the Ru surface with additional PEs. The atomic concentration of carbon can be calculated using elemental sensitivities derived empirically from standard materials,<sup>23,26,30</sup> assuming that the sensitivity factor of graphitic carbon peaking at 251 eV to be 0.281, while the Ru 231 eV peak had a sensitivity factor of 0.213.<sup>32</sup> As expected, the resulting percentages given in Table II show that AES is far more sensitive to carbon than that of XPS.

TABLE II. Relative peak-to-peak intensity ratio of the carbon and Ru Auger peaks, and the calculated at % of carbon on Ru surfaces using a relation:  $C_C = I_{251}/S_{251} \times 100 / (I_{251}/S_{251} + I_{231}/S_{231})$  where  $I_{251}$  and  $I_{231}$  are the carbon and the Ru Auger signals with respective sensitivity factors of  $S_{251} = 0.281$  and  $S_{231} = 0.213$ .

AES analyses					
Specifications	Experimental conditions	273 eV/231 eV	273 eV (top/bottom)	251 eV/201 eV	C (at.%)
Peak-to-peak intensity ratio	After sputter cleaning	2.05	0.49	0.22	14.43
	After EUV only	2.52	0.37	0.33	20.24
	After EUV with electrons	3.70	0.34	2.12	61.66

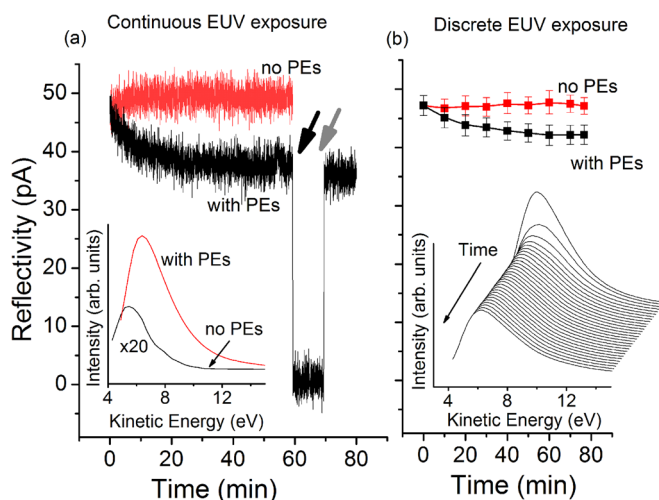


FIG. 5. (Color online) (a) EUVR of the investigating Ru mirror surface with and by screening out of PEs from the focusing Ru mirror under continuous EUV exposure, whereas (b) shows the EUVR of the Ru mirror surface in the presence and absence of additional PEs recorded by averaging over 1 min in every 10 min intervals. The black and gray arrows represents the specific times when the EUV light was switched OFF and ON, respectively. Inset (a): EUPS spectra in the cutoff region in the presence and absence of PEs from the focusing Ru mirror, where the spectrum for the latter case is multiplied by a factor 20 for clarity. Inset (b): Typical EUPS spectra recorded in 29 consecutive scans with additional PEs where each scan takes 43 s.

### C. EUV reflectivity

Figure 5(a) displays time dependent variation of the EUVR from a sputter cleaned Ru surface under continuous EUV exposure in the presence and absence of PEs from the focusing Ru mirror (stated above). Interestingly, two very different trends stand out between the data with and without screening of the additional PEs [Fig. 5(a)]. As discerned, the EUVR signal in the presence of excess PEs undergoes an exponential decay for about 30 min before stabilizing. Conversely, the measured EUVR is found to be very stable for the duration of the test by screening the additional PEs. It is important to note that the base pressure in the chamber remained similar in each experiment and the EUV source operates with a good power stability.<sup>11</sup> In order to understand the origin of the exponential decay in EUVR in presence of PEs from the focusing mirror, we measured the EUVR after halting for about 10 min at saturation (indicated by arrows: The black arrow represents where the beam was switched OFF where the gray arrow presents the time when the EUV light was switched ON again after 10 min). This result suggests that the initial exponential decay in EUVR in the presence of extra PEs is due to the effect of surface contamination. If the reflecting-PD ( $P_R$ ) was charged during data acquisition by a fraction of electrons scattered from the target surface, it should return to its initial level in absence of EUV light for 10 min, and should give similar exponential decay in EUVR when exposed to the EUV light again. However, we found that the EUVR data starts almost at the same level soon after exposing the Ru surface to the EUV light again after 10 min (indicated by gray arrow). Therefore, the change in EUVR due to charging of reflecting-PD can be ruled out. At this point, we have carried out XPS (Figs. 2

and 3) and AES (Fig. 4) to reveal the contamination level, showing the formation of a carbonaceous layer on the Ru mirror surface. Since we did not observe such exponential decay when excited with EUV radiation alone by screening out additional PEs, it seems that the EUV-induced emitted SEs from the target surface<sup>2,14</sup> are not large enough to contaminate the surface compared to the PEs from the focusing Ru mirror (see Tables I and II).

Figure 5(b) displays the measured reflectivity (averaged over 1 min) via systematic EUV exposure in the presence and absence of PEs from the focusing Ru mirror on 10 min intervals. The EUVR profile also follows an exponential decay with time in the presence of additional PEs. In contrast, the EUVR does not change much (within the error bar) and remains almost stable in absence of excess PEs. All these behavior were repeatable in different runs. Comparing these results, it appears that the driving force behind the observed decrease in EUVR in the presence of additional PEs is associated with surface contamination. A competition between oxidation and carbonization of the Ru surface is known to control the contamination level via dissociation of residual water molecules and hydrocarbons, respectively, during EUV exposure alone.<sup>2</sup> Revisiting Tables I and II, we can understand that how severe the carbon deposition is during EUV exposure in the presence of PEs from the focusing Ru mirror, and the importance of the carbonaceous layer in controlling the EUVR.

### D. EUV photoelectron spectroscopy

To justify the above results, we have also carried out EUPS measurements, basically in the low KE (cutoff) region using 13.5 nm wavelength of light. Typical cutoff region in the presence or by screening excess PEs from the focusing Ru mirror is exhibited in the inset of Fig. 5(a), showing a span of SEs emitting from the target Ru surface. The magnitude of the cutoff peak intensity is found to be almost 40 times stronger with additional PEs than that obtained by screening PEs out. Clearly, the PEs from the focusing Ru mirror actively participate in emitting such a large number of SEs from target surface. Since the SEs from the Ru mirror surface are known to play a key role in dissociating adsorbed water molecules<sup>33</sup> and hydrocarbons,<sup>2,14,34</sup> we believe that the emission of such a large number of SEs in the presence of additional PEs contribute strongly in carbon deposition (Tables I and II) with an increasing rate, though a fraction of deposited carbon atoms can be oxidized during oxidation of the underlying Ru surface and form volatile oxidized carbon species when interacting with free oxygen atoms on the Ru surface via a dissociation of water molecules.<sup>2</sup> Clearly, the carbon deposition rate in the presence of excess PEs is superior than that of oxidation-mediated desorption of carbon atoms (self-cleaning process), and thus plays a decisive role in decreasing EUVR (Fig. 5). A clear peak shift toward the higher KE region has been noticed in the presence of additional PEs [inset, Fig. 5(a)], indicating a surface charging effect because of the emission of a large number of SEs from the investigating Ru surface, that in turn gives a negative target current of  $-0.6$  nA. Moreover, when monitoring the

cutoff energy region with time in the presence of PEs from the focusing Ru mirror [inset, Fig. 5(b)], the consecutive scans of the recoded EUPS spectra (each taking 43 s) reveal a monotonic decrease in SE peak intensity until it saturates. This signifies accumulation of carbon atoms on the target surface<sup>35</sup> as the carbon layer causes a reduction of the SE yield by attenuating the migration of SEs toward the target surface, and thus the escape probability of SEs.<sup>36</sup> This is in accordance with our EUVR data [see Fig. 5(a)]. In addition, a slight fluctuation of the maximum peak position can be attributed to non-uniformity<sup>36</sup> and anisotropy<sup>6</sup> in the deposited carbon layer.

Because electrons can promote carbon growth on the Ru surface,<sup>10</sup> we conclude from the aforementioned results that the adsorption rate of carbon in the presence of additional PEs from the focusing Ru mirror is superior than the oxidation of the deposited carbon atoms by reacting with the free oxygen<sup>5</sup> from the dissociated water molecules.<sup>2</sup> Although the combination of water molecules and hydrocarbons in the chamber play an important role in the slow growth of carbon on the Ru surface under EUV radiation alone, it is shown here that the PEs from the focusing Ru mirror ultimately control the EUV-induced dissociation of hydrocarbons<sup>2,14,34</sup> and the formation of a carbonaceous Ru surface with increasing carbon deposition rate, which as a consequence decrease the EUVR (Fig. 5). Given very similar chamber conditions and source behavior during the experiments, we believe that the SEs from the studied Ru surface initiates deposition of carbon atoms via dissociation of residual hydrocarbons,<sup>34</sup> while the oxygen removal cross section for the 100 eV electrons is of the order of  $6 \times 10^{-19} \text{ cm}^2$  (Ref. 14). Moreover, the reaction rate of the deposited carbon with free oxygen can be decelerated via surface defect mediated oxidation of the Ru atoms<sup>37</sup> in time, while these reactions are associated with two simultaneous phenomena occurring at the Ru surface: (i) Background water vapor that is dissociated by the SEs can increase the free oxygen concentration and initiate oxidation of the Ru surface and (ii) breakdown of hydrocarbons can result in an increase in carbon atoms<sup>2</sup>; this can then react with free oxygen to form oxidized species of carbon<sup>2</sup> and reduce the ability of Ru substrate to adsorb/dissociate water molecules.

#### IV. SUMMARY

We investigated time dependent changes in 13.5 nm EUV reflectivity of Ru mirrors due to surface contamination. The Ru mirror surface was exposed either to continuous or discrete EUV light at regular intervals. The EUVR of sputter cleaned Ru surface decreases significantly in time in the presence of PEs from the focusing Ru mirror of our EUV setup. XPS and AES measurements were performed to analyze the change in surface composition, showing a large amount of carbon on the Ru surface when the studied Ru mirror surface was exposed to EUV light without screening out PEs from the focusing Ru mirror. As expected, AES is found to be more sensitive to determine the relative change in carbon concentration than that of XPS. By screening out excess PEs, a slight increase in carbon concentration under

EUV exposure is explained in the light of a competition between oxidation and carbonization of Ru surface via decomposition of water molecules and residual hydrocarbons, respectively. During oxidation of the Ru surface, a fraction of deposited carbon atoms can react with free oxygen and desorbs from the target Ru surface, as self-cleaning process. On the other hand, EUV-induced carbon deposition is found to be much faster and superior than the self-cleaning process in the presence of additional PEs, and thus indulges a fast decrease in EUVR. This is also consistent with the EUPS data recorded in consecutive scans, demonstrating systematic reduction in time of SEs from the target surface until it saturates in the formation of carbonaceous Ru surface. Because several mirrors will be used in any commercial EUV lithography system, our study shows screening out PEs from the successive mirror is important in mitigating surface contamination.

#### ACKNOWLEDGMENTS

This work was partially supported by SEMATECH Inc and Purdue University.

<sup>1</sup>M. Nieto, J. P. Allain, V. Titov, M. R. Hendricks, A. Hassanein, D. Rokusek, C. Chrobak, C. Tarrío, Y. Barad, S. Grantham, T. B. Lucatorto, and B. Rice, *J. Appl. Phys.* **100**, 053510 (2006).

<sup>2</sup>T. E. Madey, N. S. Faradzhev, B. V. Yakshinskiy, and N. V. Edwards, *Appl. Surf. Sci.* **253**, 1691 (2006).

<sup>3</sup>D. Campos, S. S. Harilal, and A. Hassanein, *Appl. Phys. Lett.* **96**, 151501 (2010).

<sup>4</sup>J. P. Allain, M. Nieto, M. Hendricks, S. S. Harilal, and A. Hassanein, *SPIE Proc.* **6586**, U205 (2007).

<sup>5</sup>D. J. Davis, G. Kyriakou, R. B. Grant, M. S. Tikhov, and R. M. Lambert, *J. Phys. Chem. C* **111**, 12165 (2007).

<sup>6</sup>M. Catalfano, A. Kanjilal, A. Al-Ajlony, S. S. Harilal, and A. Hassanein, *J. Appl. Phys.* **111**, 016103 (2012).

<sup>7</sup>L. Belau, J. Y. Park, T. Liang, and G. A. Somorjai, *J. Vac. Sci. Technol. B* **26**, 2225 (2008).

<sup>8</sup>R. Garg, A. Wuest, E. Gullikson, S. Bajt, and G. Denbeaux, *SPIE Proc.* **6921**, 92136 (2008).

<sup>9</sup>S. Bajt, N. V. Edwards, and T. E. Madey, *Surf. Sci. Rep.* **63**, 73 (2008).

<sup>10</sup>G. Kyriakou, D. J. Davis, R. B. Grant, D. J. Watson, A. Keen, M. S. Tikhov, and R. M. Lambert, *J. Phys. Chem. C* **111**, 4491 (2007).

<sup>11</sup>A. Egbert, B. Mader, B. Tkachenko, A. Ostendorf, C. Fallnich, B. N. Chichkov, T. Missalla, M. C. Schurmann, K. Gabel, G. Schriever, and U. Stamm, *J. Microlith. Microfabric. Microsys.* **2**, 136 (2003).

<sup>12</sup>A. Egbert, B. Tkachenko, S. Becker, and B. N. Chichkov, *SPIE Proc.* **5448**, 693 (2004).

<sup>13</sup>J. F. Moulder, W. F. Stickle, P. E. Sobol, and K. D. Bomben, *Handbook of X-ray Photoelectron Spectroscopy* (Perkin-Elmer Corporation, Eden Prairie, 1992), p. 254.

<sup>14</sup>B. V. Yakshinskiy, R. Wasielewski, E. Loginova, M. N. Hedhili, and T. E. Madey, *Surf. Sci.* **602**, 3220 (2008).

<sup>15</sup>J. Hrbek, *J. Vac. Sci. Technol. A* **4**, 86 (1986).

<sup>16</sup>K. S. Kim and N. Winograd, *J. Catalysis* **35**, 66 (1974).

<sup>17</sup>C. Stampfl and M. Scheffler, *Phys. Rev. B* **65**, 155417 (2002).

<sup>18</sup>M. Bonn, S. Funk, C. Hess, D. N. Denzler, C. Stampfl, M. Scheffler, M. Wolf, and G. Ertl, *Science* **285**, 1042 (1999).

<sup>19</sup>G. Rupprechter, V. V. Kaichev, H. Unterhalt, A. Morkel, and V. I. Bukhtiyarov, *Appl. Surf. Sci.* **235**, 26 (2004).

<sup>20</sup>A. Fohlisch, N. Wassdahl, J. Hasselstrom, O. Karis, D. Menzel, N. Martensson, and A. Nilsson, *Phys. Rev. Lett.* **81**, 1730 (1998).

<sup>21</sup>M. A. Ernst and W. G. Sloof, *Surf. Interface Anal.* **40**, 334 (2008).

<sup>22</sup>J. C. Rivière and S. Myhra, *Handbook of Surface and Interface Analysis* (CRC/Taylor & Francis Group, Boca Raton, 2009).

<sup>23</sup>D. Briggs and M. P. Seah, *Practical Surface Analysis by Auger and X-Ray Photoelectron Spectroscopy* (John Wiley, New York, 1983).

- <sup>24</sup>B. Lesiak, P. Mrozek, A. Jablonski, and A. Jozwik, *Surf. Interface Anal.* **8**, 121 (1986).
- <sup>25</sup>S. Mroczkowski and D. Lichtman, *J. Vac. Sci. Technol. A* **3**, 1860 (1985).
- <sup>26</sup>L. E. Davis, N. C. MacDonald, P. W. Plamberg, G. E. Riach, and R. E. Weber, *Handbook of Auger Electron Spectroscopy* (Physical Electronics Industries, Inc., Eden Prairie, 1976).
- <sup>27</sup>M. J. van Staden and J. P. Roux, *Appl. Surf. Sci.* **44**, 259 (1990).
- <sup>28</sup>D. W. Goodman and J. M. White, *Surf. Sci.* **90**, 201 (1979).
- <sup>29</sup>R. Pfandzelter, G. Steierl, and C. Rau, *Phys. Rev. Lett.* **74**, 3467 (1995).
- <sup>30</sup>J. M. Walls, *Methods of Surface Analysis* (Press Syndicate of the University of Cambridge, New York, 1989).
- <sup>31</sup>M. J. Vanstaden and J. P. Roux, *Appl. Surf. Sci.* **44**, 259 (1990).
- <sup>32</sup>P. W. Palmberg, *Handbook of Auger Electron Spectroscopy: A Reference Book of Standard Data for Identification and Interpretation of Auger Electron Spectroscopy Data*, 2nd ed. (Physical Electronics, Eden Prairie, Minnesota, 1976).
- <sup>33</sup>J. Hollenshead and L. Klebanoff, *J. Vac. Sci. Technol. B* **24**, 118 (2006).
- <sup>34</sup>J. Hollenshead and L. Klebanoff, *J. Vac. Sci. Technol. B* **24**, 64 (2006).
- <sup>35</sup>A. Septier and M. Belgaroui, *IEEE Trans. Electric. Insulation* **EI-20**, 725 (1985).
- <sup>36</sup>J. Chen, E. Louis, J. Verhoeven, R. Harmsen, C. J. Lee, M. Lubomska, M. van Kampen, W. van Schaik, and F. Bijkerk, *Appl. Surf. Sci.* **257**, 354 (2010).
- <sup>37</sup>R. Blume, H. Niehus, H. Conrad, and A. Böttcher, *J. Phys. Chem. B* **108**, 14332 (2004).